Time Course of the Initial $[Ca^{2+}]_i$ Response to Extracellular ATP in Smooth Muscle Depends on $[Ca^{2+}]_e$ and ATP Concentration

Mỹ G. Mahoney,* Linda L. Slakey,* Christopher D. Benham,# and David J. Gross*
*Program in Molecular and Cellular Biology and Department of Biochemistry and Molecular Biology, University of Massachusetts, Amherst, Massachusetts 01003, USA, and #SmithKline Beecham Pharmaceuticals, Harlow, Essex CM19 5AW, England

ABSTRACT In response to extracellular application of 50 μM ATP, all individual porcine aortic smooth muscle cells respond with rapid rises from basal $[Ca^{2+}]_i$ to peak $[Ca^{2+}]_i$ within 5 s. The time from stimulus to the peak of the $[Ca^{2+}]_i$ response increases with decreasing concentration of ATP. At ATP concentrations of 0.5 μM and below, the time to the $[Ca^{2+}]_i$ peak varies more significantly from cell to cell than at higher concentrations, and each cell shows complicated initiation and decay kinetics. For any individual cell, the lag phase before a response decreases with increasing concentration of ATP. An increase in lag time with decreasing ATP concentration is also observed in the absence of extracellular Ca^{2+}, but the lag phase is more pronounced, especially at concentrations of ATP below 0.5 μM. Whole-cell patch-clamp electrophysiology shows that in porcine aortic smooth muscle cells, ATP stimulates an inward current carried mainly by Cl^- ion efflux with a time course similar to the $[Ca^{2+}]_i$ changes and no detectable current from an ATP-gated cation channel. A simple signal cascade initiation kinetics model, starting with nucleotide receptor activation leading to IP_3-mediated Ca^{2+} release from IP_3-sensitive internal stores, fits the data and suggests that the kinetics of the Ca^{2+} response are dominated by upstream signal cascade components.

INTRODUCTION

Dependence of the initiation time for a $[Ca^{2+}]_i$ response on the concentration of extracellular agonists has been shown recently for several cell-agonist pairs (Cheyette and Gross, 1991; Droogmans et al., 1991; Kalthof et al., 1993; Meyer et al., 1990). Two observations common to these studies were that the time between stimulus and $[Ca^{2+}]_i$ response increases with decreasing concentrations of agonist and that the time to $[Ca^{2+}]_i$ peak as well as the magnitude of the response varies from cell to cell. For epidermal growth factor and A431 cells, the kinetics and onset of the $[Ca^{2+}]_i$ response were predicted well by a model that assumed a cascade of cellular second messenger events leading from receptor activation to Ca^{2+} release from internal Ca^{2+} stores (Cheyette and Gross, 1991).

We have shown that individual pig aortic smooth muscle cells respond to extracellular ATP in a concentration-dependent manner with an initial transient rise followed by oscillations in $[Ca^{2+}]_i$ that are asynchronous from cell to cell (Mahoney et al., 1992). The initial transient rise in $[Ca^{2+}]_i$ rapidly desensitizes, and most of the change in $[Ca^{2+}]_i$ derives from internal Ca^{2+} store release (Kalthof et al, 1993; Mahoney et al., 1992). Extracellular ATP has been shown to stimulate IP_3 formation, which subsequently releases Ca^{2+} from IP_3-sensitive intracellular Ca^{2+} pools (Kalthof et al., 1993; Tawada et al., 1987). Results from freshly isolated rabbit ear artery smooth muscle cells suggest that influx of extracellular Ca^{2+} via ATP-activated Ca^{2+} permeable channels (Benham, 1989; Benham and Tsien, 1987) also plays a role in the generation of the initial cytosolic calcium transient rise. Whereas this channel shows low Ca^{2+} permeability relative to voltage-gated Ca^{2+} channels, under physiological Na^+ and Ca^{2+} transmembrane ion gradients, significant $[Ca^{2+}]_i$ rises are generated by flux through this channel (Benham, 1989). However, cultured pig aortic smooth muscle cells display an inward current due to Cl^- efflux in response to extracellular ATP (Droogmans et al., 1991). Although this inward current is carried principally by Cl^-, a smaller contribution of the total current from nonselective cation channels cannot be completely ruled out. Hartley and Kozlowski (1997) have shown that ATP stimulation of rat pulmonary artery smooth muscle cells induces an initial transient inward current carried predominantly by cations and mediated by a P_{2X} receptor, followed by oscillatory inward current carried predominantly by chloride ion and mediated by a P_{2U} receptor. Cloning of cDNAs encoding families of P_{2X} receptor ligand-gated cation channels and G-protein coupled P_{2Y} and P_{2U} receptors has aided the identification of the molecular constituents of the transduction pathways (reviewed by North and Barnard, 1997).

In this report, a digital fluorescence imaging system was used to measure the temporal changes in intracellular free calcium in individual adherent cells that were loaded with the calcium-sensitive indicator fura-2. The time course and the cell-to-cell variability of the initial rise in $[Ca^{2+}]_i$ in response to varying concentrations of ATP in the presence and absence of extracellular Ca^{2+} were shown to increase with decreasing ATP concentration. This effect was en-

Received for publication 5 January 1998 and in final form 22 June 1998.

Address reprint requests to Dr. David J. Gross, Department of Biochemistry and Molecular Biology, Graduate Research Tower, University of Massachusetts, Amherst, MA 01003. Tel.: 413-545-3170; Fax: 413-545-3291; E-mail: dgross@biochem.umass.edu.

Dr. Mahoney's present address is Department of Dermatology, University of Pennsylvania Medical School, Philadelphia, PA 19104.

0006-3495/98/10/2050/09 $2.00

hanced by the removal of extracellular Ca^{2+}, a novel finding that initially suggested that Ca^{2+} influx mediated by nucleotide receptor activation plays a significant role in the initial cellular ionic response to extracellular ATP. Whole-cell electrophysiology was used to determine the contribution of the influx of external calcium to the initial rise in $[Ca^{2+}]_i$. Surprisingly, removal of extracellular Ca^{2+} in consort with strong buffering of intracellular $[Ca^{2+}]_i$ with EGTA completely abolished ATP-activated ion currents, demonstrating that no P_{2X} receptor activity contributes to ATP-activated ion signaling in pig aorta smooth muscle cells, in contrast to the role of a P_{2X} receptor in rat pulmonary artery smooth muscle cells (Hartley and Kozlowski, 1997). Ion substitution experiments demonstrated that a Ca^{2+}-activated Cl^- current dominated the transmembrane ion flux in response to ATP stimulation of pig aorta smooth muscle cells, suggesting that both the initial transient and subsequent oscillations of transmembrane ion flux found in response to ATP stimulation were driven by $[Ca^{2+}]_i$ signals that we have previously characterized (Mahoney et al., 1992). A simple model based on an IP_3-mediated signaling cascade initiated by nucleotide receptor activation was found to describe the kinetics of the initial change in $[Ca^{2+}]_i$.

MATERIALS AND METHODS

Smooth muscle cell culture

Vascular smooth muscle cells were isolated from minced medial tissue of pig aorta incubated at 37°C overnight in Dulbecco's modified Eagle's medium (DME) (Gibco, Grand Island, NY) supplemented with 0.3% collagenase (Goldman et al., 1983; Linderman et al., 1989). The digest was centrifuged (3000 rpm for 2 min), and the pellet was resuspended in a growth medium consisting of DME supplemented with 200 units/ml penicillin, 0.2 mg/ml streptomycin, and 10% fetal calf serum, and plated in a T-25 flask. This primary cell culture was allowed to grow to confluency (7–10 days) in serum-containing growth medium at 37°C in a 5% CO_2/95% air atmosphere. Serial subcultures (1:4) were prepared by trypsinization with 0.05% trypsin/versene solution. Experiments were performed on cells between passages 3 and 15. Approximately 1–2 $\times$ 10^5 cells were seeded onto 35-mm culture dishes (for electrophysiology) or no. 1 glass coverslips in 35-mm culture dishes (for the Ca^{2+} detection experiments). Each day thereafter, the cells were fed with DME supplemented with 0.5 μg/ml transferrin, 0.6 μg/ml insulin, and 0.04 mg/ml ascorbic acid (defined medium) (Libby and O'Brien, 1983; Xiong et al., 1991). Experiments were performed 72 h after final plating onto coverslips.

Measurements of $[Ca^{2+}]_i$ in single cells

Cells were loaded with 2 μM fura-2 acetoxymethylester (fura-2/AM) (Molecular Probes, Eugene, OR) plus 0.02% pluronic F-127 in HEPES-buffered saline (HBS) (20 mM HEPES (pH 7.4), 125 mM NaCl, 5.4 mM KCl, 1.8 mM $CaCl_2$, 0.8 mM $MgSO_4$, 5.5 mM D-glucose) with 0.3% dimethylsulfoxide for 30 min at 37°C. The coverslip was then washed with HBS and mounted in a flow chamber held at 37°C. The volume of the cell chamber was 0.8 ml. Approximately 2.5 ml of agonist in HBS at 37°C was introduced into the flow chamber reservoir as previously described (Linderman et al., 1989). Solution exchange was more than 80% complete within 1 s and reached 95% in less than 4 s (Cheyette and Gross, 1991).

To maximize temporal resolution for most experiments, fluorescence images were captured with excitation at a single wavelength (334 nm; Ca^{2+}-sensitive wavelength) every second. The addition of an agonist to the cell chamber was made between two image frames. The time of the image frame immediately after the addition was defined as $t = 0$. Calcium-free HBS had 100 μM EGTA in place of the $CaCl_2$; ~5.0 ml was required to completely remove the calcium when the chamber previously contained standard HBS. Results in Fig. 2 and Table 1 include experiments performed with two excitation wavelengths as previously described (Mahoney et al., 1992), with 2-s temporal resolution.

In some experiments, Ca^{2+} was removed from the extracellular medium by washing cells three times in Ca^{2+}-free HBS plus 100 μM EGTA. The cells were exposed to this Ca^{2+}-free medium for ~20 s. Under identical conditions, these cells suffered a barely detectable decrease in $[Ca^{2+}]_i$ from ~100 nM to 95 nM as previously reported (Mahoney et al., 1992). It is unlikely that intracellular Ca^{2+} stores were depleted to a significant extent by this treatment. To further minimize depletion of Ca^{2+} stores in cells that were stimulated multiple times, ATP was applied sequentially from lowest to highest concentration. Cells were allowed to rest in Ca^{2+}-containing HBS for 5 min between ATP applications. This protocol has previously been shown to allow cells to fully recover responsiveness between ATP applications (Mahoney et al., 1992).

Electrophysiology

Cells were bathed in an extracellular milieu of 125 mM NaCl, 5 mM KCl, 1 mg/ml glucose, 0.8 mM $MgCl_2$, 1.8 mM $CaCl_2$, and 20 mM HEPES (buffered to pH 7.3 with NaOH). The intracellular (pipette filling) solution contained 125 mM CsCl, 2.6 mM $MgCl_2$, 10 mM HEPES, and 100 μM EGTA (buffered to pH 7.3 with CsOH). In experiments in which chloride was removed from the extracellular solution, Na-isethionate replaced part or all of the NaCl. Electrophysiology experiments were performed at room temperature (~22°C). Voltage clamp recordings were made with a List EPC-7 patch-clamp amplifier as previously described (Benham, 1989; Hamill et al., 1981). Voltage steps were produced with a step command generator (University of Newcastle) triggered by a Digitimer. Membrane potential and current signals were passed through a modified Sony PCM 701 digital audio processor (Lamb, 1985) and stored on digital audiotape.

RESULTS

Effect of ligand concentration on the time course of the initial $[Ca^{2+}]_i$ rise

In response to 125 nM ATP, the lag time and the magnitude of the initial rise in $[Ca^{2+}]_i$ varied dramatically from cell to cell, as shown in Fig. 1. In this figure, 12 cells on the same coverslip were stimulated with 125 nM ATP in the absence of extracellular Ca^{2+}. Of the 12 cells, eight responded with robust $[Ca^{2+}]_i$ rises that peaked at 26, 32, 48, 52, 68, 71, 72, and 81 s after stimulation. The other four cells responded with a slight increase in $[Ca^{2+}]_i$, with a delay time to $[Ca^{2+}]_i$ peak of greater than 80 s. A subsequent stimulation with a higher concentration of ATP (50 μM) caused a robust $[Ca^{2+}]_i$ rise in each cell that was more nearly synchronous among all of the cells, peaking at ~2–10 s after ATP stimulation. The slope of the steepest portion of the $[Ca^{2+}]_i$ rise was significantly steeper at 50 μM ATP than at 125 nM. This figure demonstrates that for any group of cells, the time to peak $[Ca^{2+}]_i$ response increases with decreasing concentration of ATP.

Next, the time course of initiation of the rise of $[Ca^{2+}]_i$ in individual cells stimulated with various concentrations of ATP was examined. Cells were allowed to recover for 5 min

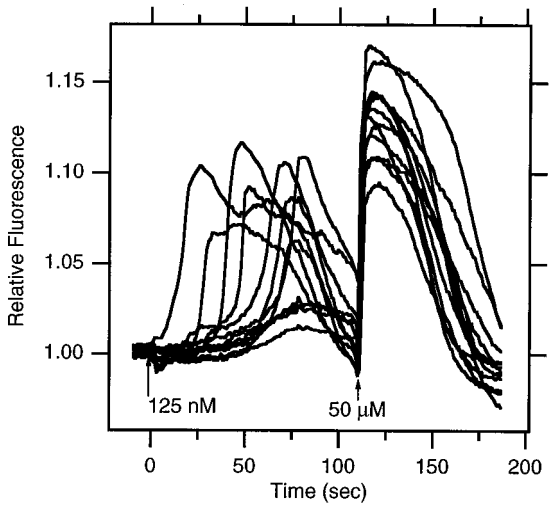

FIGURE 1 Effect of ligand concentration on the time course and shape of the initial $[Ca^{2+}]_i$ rise. Twelve cells incubated in HBS + 100 μM EGTA without Ca^{2+} were stimulated with 125 nM ATP followed by 50 μM ATP as marked with arrows. The fluorescence of all cells was normalized to the prestimulus level. Data were taken at 334-nm excitation only to maximize image collection speed.

after each ATP stimulus. We have shown previously that the $[Ca^{2+}]_i$ response reproducibly recovers from an ATP stimulus over this time course (Mahoney et al., 1992). A representative cell shown in Fig. 2 responded to 125 nM ATP with a slow rise in cytosolic calcium $[Ca^{2+}]_i$, peaking ~40 s after ATP stimulation. When stimulated with 250 nM ATP, the same cell responded with an explosive transient rise in $[Ca^{2+}]_i$, peaking at 27 s. The times to peak $[Ca^{2+}]_i$ were reduced to 12 and 4 s for 500 nM and 50 μM ATP, respectively. Similar results were seen for more than 50 other cells, although the absolute lag times and response amplitudes varied from cell to cell.

Four individual cells on the same coverslip were stimulated with 50 nM, 500 nM, and 5 μM ATP (Fig. 3). When exposed to 50 nM ATP (Fig. 3 *A*), only cells 1 and 2 showed a slow rise in $[Ca^{2+}]_i$, peaking at 22–26 s, whereas the other cells did not respond. The cells were then washed three

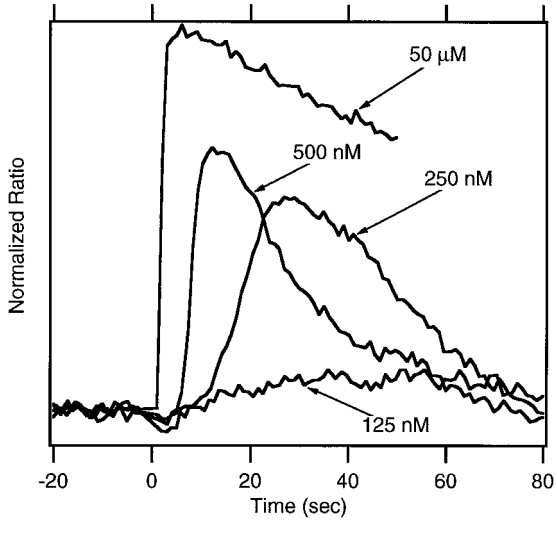

FIGURE 2 Time to the peak $[Ca^{2+}]_i$ response decreases with an increasing ATP concentration. A representative cell is stimulated with four concentrations (125 nM, 250 nM, 500 nM, and 50 μM) of ATP, with a 5-min resensitization period between stimulation periods. Fura-2 data were taken as 334-nm and 365-nm excitation image pairs (Mahoney et al., 1992). The 334 nm/365 nm fluorescence ratio traces were normalized to the prestimulus level and were overlapped to the time of ATP addition. Time to $[Ca^{2+}]_i$ peak; 125 nM > 40 s, 250 nM = 27 s, 500 nM = 12 s, and 50 μM = 4 s.

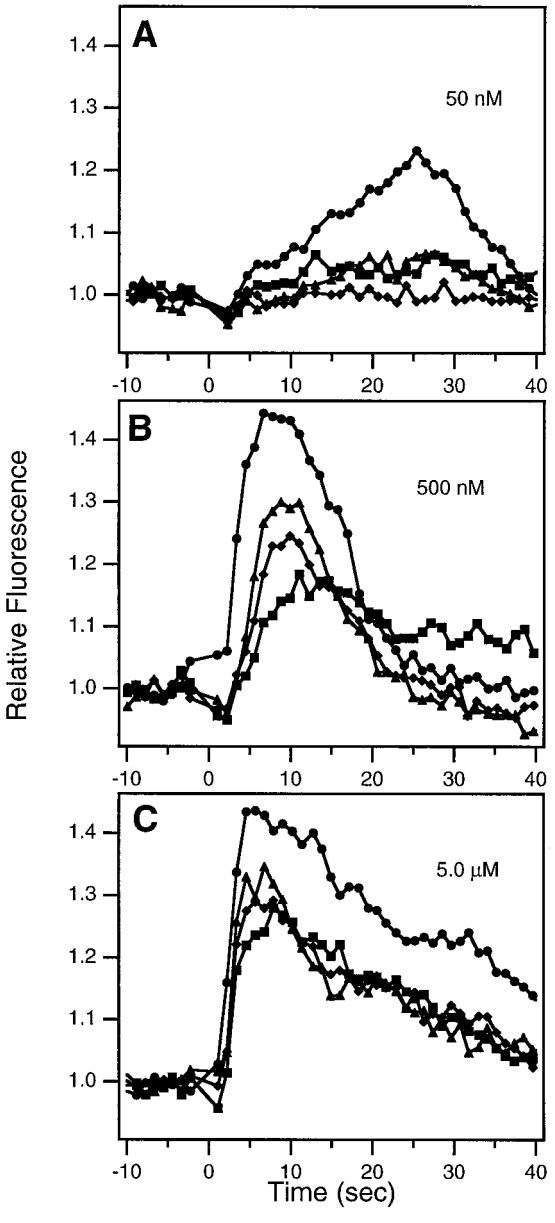

FIGURE 3 Cell-to-cell variation in the time course of the initial $[Ca^{2+}]_i$ rise. Four representative cells shown here were stimulated with 50 nM (*A*), 500 nM (*B*), and 5.0 μM (*C*) ATP with HBS washes and a 5-min resensitization period between stimulation periods. The fluorescence traces were normalized to the prestimulus level and were overlapped to the time of ATP addition. ●, cell 1; ▲, cell 2; ◆, cell 3; ■, cell 4.

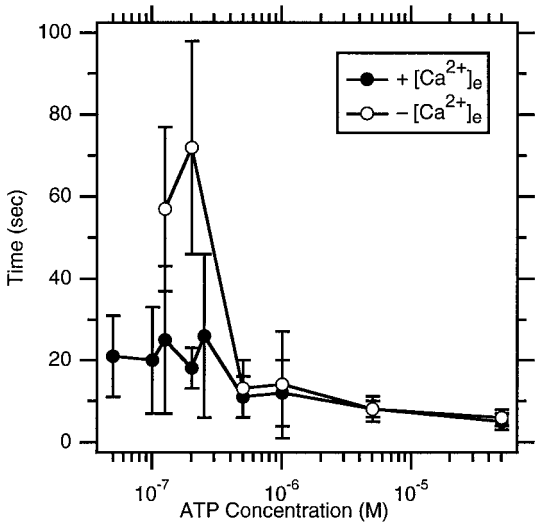

FIGURE 4 Concentration dependence of time to peak $[Ca^{2+}]_i$ response in the presence and absence of extracellular Ca^{2+}. Mean values with standard deviation error bars of the time to peak $[Ca^{2+}]_i$ of 720 smooth muscle cells stimulated with various concentrations of ATP in the presence (●) or absence (○) of extracellular Ca^{2+}.

times with HBS to remove the ATP and were allowed to rest for 5 min. The cells were then stimulated with 500 nM ATP, for which the initial transient rises began after an ~2-s delay in all cells. The times to peak $[Ca^{2+}]_i$ response of cells 1–4 were 7, 9, 10, and 11 s, respectively. The cells were again washed with HBS, allowed to rest for a further 5 min, and stimulated with 5 μM ATP. The times to peak $[Ca^{2+}]_i$ response for the four cells were 5, 5, 6, and 8 s, respectively. The data show that at all agonist concentrations, the magnitude and time course of the $[Ca^{2+}]_i$ rise vary from cell to cell, and that the relative responsiveness of the individual cells maintained at the same rank order across a 100-fold agonist concentration range.

Modulation of the response to ATP by extracellular Ca^{2+}

The influence of extracellular Ca^{2+} on the sensitivity of the initiation of the $[Ca^{2+}]_i$ response to ATP was examined. Fig. 4 shows the mean values with standard deviation of the time to peak $[Ca^{2+}]_i$ of 720 individual cells responding to various concentrations of ATP in the presence or absence of external Ca^{2+}. In the presence of extracellular Ca^{2+}, the average time to peak $[Ca^{2+}]_i$ decreases, and the cell-to-cell variability decreases with increasing concentration of ATP. In the absence of external Ca^{2+}, the cell-to-cell variability also converges, and the average time to peak $[Ca^{2+}]_i$ decreases with an increasing concentration of ATP. At concentrations higher than 500 nM ATP, the average times to peak $[Ca^{2+}]_i$ are only slightly faster in the presence than in the absence of external Ca^{2+}. However, at concentrations of ATP lower than 500 nM, the average time to peak response increases in the absence of external Ca^{2+} compared to the presence of external calcium (statistically significant Student's *t*-test; $p < 0.005$ at 125 nM and 200 nM ATP) (Table 1).

When the responses of individual cells in the presence and absence of extracellular Ca^{2+} are examined, differences in the lag time are apparent even at 500 nM ATP. Although the population average response at ATP stimulus levels of 500 nM is only modestly different in the presence and absence of extracellular Ca^{2+} (Fig. 4), comparing these response times in the same cell demonstrates that the absence of extracellular Ca^{2+} slows the $[Ca^{2+}]_i$ response. In the presence of 1.8 mM external Ca^{2+}, the cytosolic $[Ca^{2+}]_i$ transients (*filled circles*) in three cells peaked at 5, 5, and 3 s after the addition of 500 nM ATP (Fig. 5). The external ATP was removed and the cells were allowed to recover for 5 min in HBS containing Ca^{2+}. External calcium was removed for ~20–30 s by rinses with HBS without calcium plus 100 μM EGTA. We have previously shown that removal of extracellular Ca^{2+} by exposure of these cells to

TABLE 1 Time to peak $[Ca^{2+}]_i$ rise in response to extracellular ATP

	+ extracellular Ca^{2+}		− extracellular Ca^{2+}	
[ATP] (μM)	Time to $[Ca^{2+}]_i$ peak (s)	No. responded/ total no. cells	Time to $[Ca^{2+}]_i$ peak (s)	No. responded/ total no. cells
0.05	21 ± 10	(4/58)		(0/31)
0.1	20 ± 13	(6/49)	46	(1/45)
0.125	25* ± 18	(17/40)	57* ± 20	(8/15)
0.2	18** ± 5	(6/30)	72** ± 26	(10/42)
0.25	26 ± 20	(6/39)		(0/17)
0.5	11 ± 5	(65/93)	13 ± 7	(25/50)
1	12 ± 8	(20/34)	14 ± 13	(23/32)
5	8 ± 3	(47/47)	8 ± 2	(16/16)
50	5 ± 2	(46/46)	6 ± 2	(36/36)

Individual porcine aortic smooth muscle cells were loaded with fura-2/AM and were stimulated with varying concentrations of ATP in the presence or absence of extracellular Ca^{2+}. The time to peak $[Ca^{2+}]_i$ was determined. Some of these experiments were performed with fluorescence detected only at 334-nm excitation wavelength (resolution = 1 s) and some with dual wavelength detection (resolution = 2 s). The fraction of cells that respond at low [ATP] (<250 nM) is quite variable. This is to be expected, based on counting statistics in which the relative uncertainty in counting a small number N of events is $\sqrt{N}$. For example, at 0.2 μM ATP, one would expect uncertainties of ±2.4 and ±3.2 responding cells for the Ca^{2+}-containing and Ca^{2+}-free data, respectively.

*,**Significantly different ± $[Ca^{2+}]_e$ (Student's t-test; $p < 0.005$).

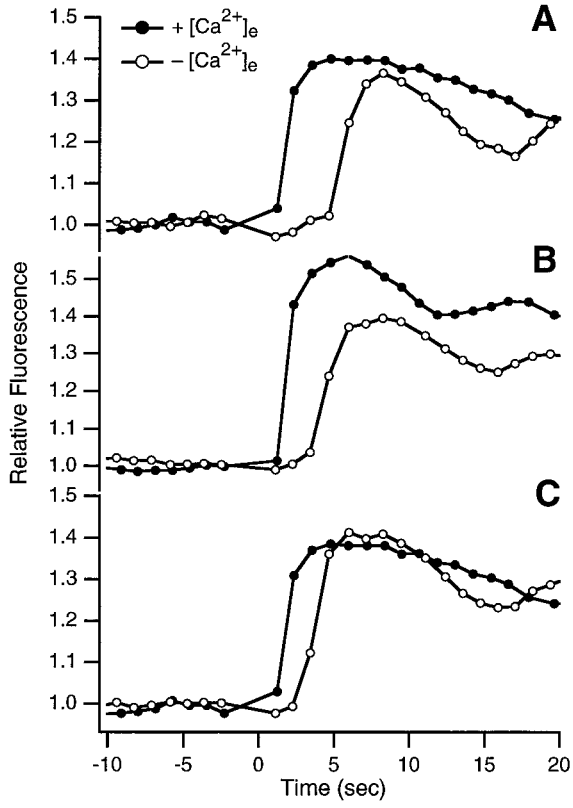

FIGURE 5 Extracellular Ca^{2+} removal delays the time to a $[Ca^{2+}]_i$ response to ATP. In the presence of 1.8 mM external Ca^{2+}, these three representative cells were stimulated with 500 nM ATP. The external ATP was removed, and the cells were allowed to recover for 5 min in HBS containing 1.8 mM Ca^{2+}. Next, external Ca^{2+} was removed by rinses with HBS + 100 μM EGTA without Ca^{2+}. The same cells were then stimulated with 500 nM ATP in the absence of extracellular Ca^{2+}. The two fluorescence traces were normalized to the prestimulus level and were overlapped to the time of ATP addition.

HBS plus 100 μM EGTA induces a very small decrease in $[Ca^{2+}]_i$ from ~100 nM to ~95 nM (figure 6 in Mahoney et al., 1992). The same cells were then stimulated with 500 nM ATP in HBS without calcium (*open circles*). The second stimulus $[Ca^{2+}]_i$ transients showed, respectively, an increased time to peak response of 8, 6, and 6 s after ATP addition. This increase in time to initiation of the $[Ca^{2+}]_i$ rise as well as to peak $[Ca^{2+}]_i$ indicates that extracellular Ca^{2+} modulates the initiation rate of the cytosolic calcium response to ATP. That this slowing of the $[Ca^{2+}]_i$ response was not due to Ca^{2+} store depletion is suggested by analysis of the peak heights of the individual cell responses in Fig. 5. The ratio of the peak response amplitudes ($+Ca^{2+}/-Ca^{2+}$) for these three cells is 1.04 ± 0.07. If the detected amplitude of the $[Ca^{2+}]_i$ response is proportional to the extent of Ca^{2+} store filling, this result suggests that exposure of the cells to Ca^{2+}-free medium did not deplete the stores.

ATP-stimulated plasma membrane currents

Next, we determined whether pig aortic smooth muscle cells display Ca^{2+} influx through ATP-gated cation channels similar to those observed in freshly isolated rabbit ear artery cells (Benham and Tsien, 1987) or other cell types (for a review, see Bean and Friel, 1990). If such a current exists in these cells, it could contribute to the difference in the onset of the rise of $[Ca^{2+}]_i$ in the presence and absence of extracellular Ca^{2+}. In voltage-clamped arterial smooth muscle cells at a holding potential of −40 mV, ATP (10 μM) produced a transient inward current with a time course similar to that of the current observed by Droogmans et al. (1991). In a number of cells repetitive oscillations in inward current were observed on continued application of ATP (Fig. 6). The average magnitude of the ATP-stimulated inward current was 360 ± 110 pA (mean ± SD; n = 8 cells). These currents were measured in cells filled with

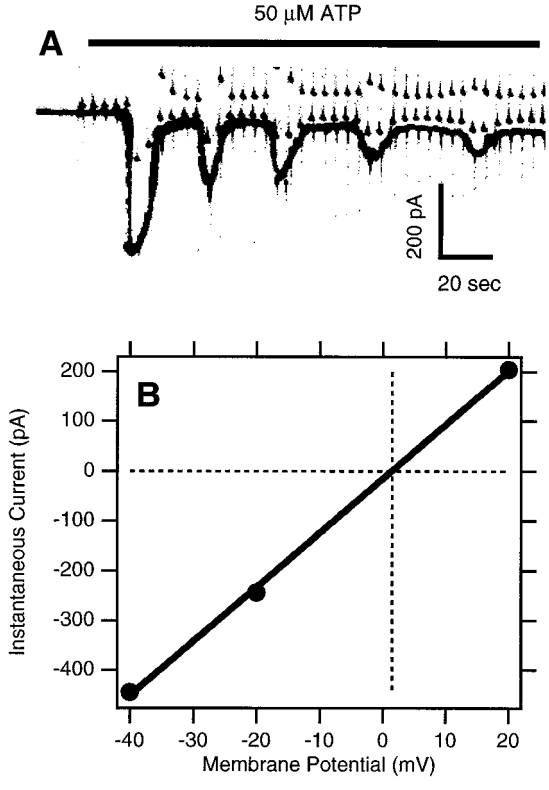

FIGURE 6 Initial transient and oscillations of inward current in response to extracellular ATP. (*A*) Whole-cell recording of plasma membrane current for a voltage-clamp experiment. During the continuous recording, the membrane potential was stepped from −40 mV (3200 ms) to −20 mV (400 ms) to +20 mV (400 ms) and returned to −40 mV. The cycle was then repeated. ATP (50 μM) was applied as shown with the bar above the current trace. Much of the latency to response after ATP application reflects dead time in the exchange flow system. Pipette solution in mM: 147.7 KCl, 1 $MgCl_2$, 0.1 EGTA, 10 HEPES, pH 7.4. Bathing solution in mM: 125 NaCl, 5 KCl, 0.8 $MgCl_2$, 1.8 $CaCl_2$, pH 7.4. Scale bars: *vertical*, 200 pA (*downward* is inward current); *horizontal*, 20 s. (*B*) Plot of the instantaneous current measured from the data in *A* versus the membrane voltage. The instantaneous current at −40, −20, and +20 mV was measured by subtracting the current detected before ATP stimulation from the current detected at the stable part of the peak of the ATP-stimulated inward ion flux (*filled circles*); the current-voltage relationship was fit by linear regression (*solid line*). The instantaneous inward current reverses at +1.5 mV (*dashed lines*). Similar results were observed in seven cells.

pipette solution containing 100 μM EGTA and bathed in normal HBS. We next performed a number of experiments with cells filled with pipette solution containing 11 mM EGTA and bathed in Ca-free HBS plus 100 μM EGTA to investigate the dependence of this current on $[Ca^{2+}]_i$. In four experiments under these conditions 10 μM ATP failed to evoke any inward current. In $[Ca^{2+}]_i$ measurement experiments with fura-2, microinjection of 100 mg/ml heparin completely abolished any $[Ca^{2+}]_i$ changes in response to ATP, suggesting that a rise in IP_3 is crucial for mediating the $[Ca^{2+}]_i$ transient ($n = 2$ cells). When 1 mg/ml heparin was included in the internal pipette solution for electrophysiology, the ATP-stimulated inward current amplitude was substantially reduced (to 72%; $n = 3$ cells). Taken together, these data strongly suggest that all of the inward current observed was dependent upon elevation of $[Ca^{2+}]_i$.

Further experiments were designed to investigate the permeant ions in these Ca^{2+}-activated currents. To determine the reversal potential of the current, the membrane potential was cyclically stepped from -40 mV (3200 ms) to -20 mV (400 ms) to $+20$ mV (400 ms) continuously during the experiment. At a relatively stable part of the initial inward current near its peak, the reversal potential was measured by plotting the instantaneous current versus membrane potential. The reversal potential of the ATP-mediated current in the presence of 150 mM Cl^- inside and 135 mM Cl^- outside of the cell was -5 ± 5 mV ($n = 8$). Table 2 summarizes the reversal potentials of membrane current responses to extracellular ATP at various Cl^- concentrations. The replacement of Cl^- with isethionate in the extracellular bathing solution shifted the reversal potential to $+20 \pm 9$ mV ($n = 4$). The positive shift in E_{rev} was consistent with Cl^- ions contributing to current flow, but less than expected if all of the current was carried by Cl^- ions. This suggests that another conductance contributed to the ATP-elicited current. The most likely candidate is a nonselective cation conductance activated by Ca^{2+} released by ATP stimulus rather than directly by extracellular ATP. Such a channel would have E_{rev} close to zero mV under the above conditions and thus would limit E_{rev} shifts due to Cl^- replacement. Incomplete abolition of a Ca^{2+}-activated K^+ current under these conditions cannot be excluded as a partial explanation, although the lack of a large effect of exchanging internal K^+ for Cs^+ (Fig. 6 and Table 2) indicates that this is unlikely to be the dominant contaminating current.

TABLE 2 Reversal potentials of ATP-induced current

External solution $[Cl^-]$ (mM)	Internal solution $[Cl^-]$ (mM)	E_{rev} mean $\pm$ SD (mV)	n
149	130	-5 ± 5	8
75	130	4 ± 4	4
10	130	20 ± 9	4
10	0	32 ± 5	8

The intracellular (pipette filling) solution contained 125 mM CsCl, 2.6 mM $MgCl_2$, 10 mM HEPES, and 100 μM EGTA (buffered to pH 7.3 with CsOH). The cells were then stimulated with 10 μM ATP in an extracellular milieu of 125 mM NaCl, 5 mM KCl, 5.5 mM glucose, 0.8 mM $MgCl_2$, 1.8 mM $CaCl_2$, and 20 mM HEPES (buffered to pH 7.3 with NaOH). In experiments in which chloride was removed from the extracellular or intracellular solutions, Na-isethionate replaced NaCl and Cs-aspartate replaced CsCl. All experiments were performed at room temperature (~22°C).

n, Number of cells examined.

The apparent lack of P_{2X} receptor-mediated currents is unlikely to be due to inactivation of P_{2X} receptors during the course of ATP application in these experiments. The solution exchange system used here was quite similar to that employed by Benham (1989). In that study, freshly dissociated vascular cells displayed P_{2X}-mediated Ca^{2+} currents in response to 1–10 μM ATP. Similar currents would have been readily detectable in the present experiments. Thus these pig aortic smooth muscle cells do not express functional P_{2X}-mediated Ca^{2+}-permeable channels.

DISCUSSION

We have shown that the time course and magnitude of the ATP-stimulated $[Ca^{2+}]_i$ rise in pig aorta smooth muscle cells vary from cell to cell, and that the variability of the timing of the response increases with decreasing ATP concentration, whereas the amplitude of the response decreases. Furthermore, extracellular Ca^{2+} has been shown to modulate the initiation of the $[Ca^{2+}]_i$ response to ATP. That the lag time to the initial $[Ca^{2+}]_i$ response increases with decreasing ATP concentration is observed at the individual cell level for a large number of cells. The mean time to peak $[Ca^{2+}]_i$ decreases from ~21 s to 6 s for ATP concentrations ranging from 50 nM to 50 μM. At low concentrations of ATP, 125 nM and 200 nM, the lag time in the absence of extracellular Ca^{2+} increases by about threefold compared to that in the presence of extracellular Ca^{2+}.

The increase in time between ATP stimulus and $[Ca^{2+}]_i$ response is consistent with the sequential pathway of signal transduction thought to mediate this response. A cascade of activation signals leading from nucleotide receptor through a G-protein to phospholipase C (PLC) activation followed by production of inositol 1,4,5-trisphosphate (IP_3) and release of Ca^{2+} from IP_3-sensitive stores appears to mediate the process (Kalthof et al., 1993; Mahoney et al., 1992). Such a signal cascade can produce $[Ca^{2+}]_i$ signals that appear explosively after a significant lag time after ligand stimulus (Cheyette and Gross, 1991).

The delay between exogenous ATP stimulus and the subsequent $[Ca^{2+}]_i$ response described in the Results was analyzed based on a simple signal cascade model. This model was stripped of all components that involve stabilizing, reverse reactions and that contain dependencies on $[Ca^{2+}]_i$. Thus this model is applicable only at the earliest phase of a response to ATP. Despite its simplicity, it predicts the general features of the cellular response, although by its simplicity it is limited in its capacity for quantitative prediction.

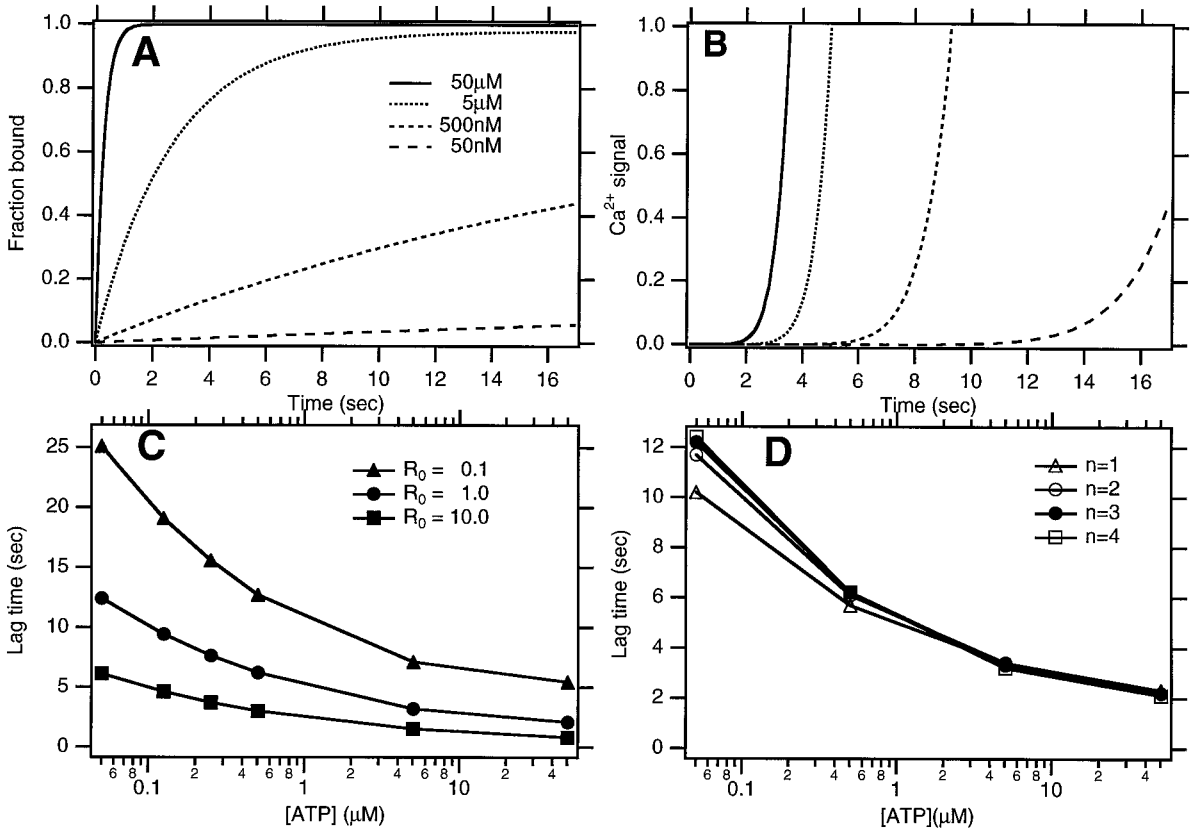

FIGURE 7 Predicted kinetics of ligand binding and $[Ca^{2+}]$ response based on a catalytic cascade signal transduction pathway. (*A*) Fraction of receptors occupied versus time for four [ATP]. (*B*) Time course of the response (increase in $[Ca^{2+}]_i$ above baseline) for each of the [ATP] of *A*. The vertical scale is in arbitrary units. Because no reverse reactions or dissipative elements are included in the model, the Ca^{2+} signal never decreases; thus this model is valid only for early times in the signal process. (*C*) Concentration dependence of the time between stimulus ($t = 0$) and response (lag time). The response was defined to occur at the time at which the Ca^{2+} signal reached 0.2 on the scale of *B*. The relative number of cell surface receptors was varied over two orders of magnitude, as indicated in the inset. (*D*) Dependence of the lag time (as in *C*) on the Hill coefficient n for IP_3-mediated Ca^{2+} release.

For the model, ATP was presumed to bind to its receptor monovalently with an equilibrium dissociation constant of $K_D = 0.11\ \mu M$ (Mahoney et al., 1992). The forward rate constant of the ligand-receptor binding reaction, k_f, was assumed to be equal to that found by Boyer et al. (1990) for 3′-*O*-(4-benzoyl)benzoyl ATP binding to turkey erythrocyte plasma membranes, $7.41 \times 10^{-2}\ \mu M^{-1}\ s^{-1}$. The reverse rate constant, k_r, was calculated from the assumed k_f and K_D to be $8.15 \times 10^{-3}\ s^{-1}$. Given these rate constants, the time course of accumulation of ligand-bound receptors with a step increase in ligand concentration as a function of ligand concentration L is

$$[LR] = \{1 - e^{-t/\tau}\}R_0/(1 + K_D/L)$$

where $\tau = (k_f L + k_r)^{-1}$, and R_0 is the concentration of total receptors on a cell. The fraction of receptors bound versus time for four concentrations of extracellular ATP is shown in Fig. 7 *A*.

Given the assumptions that several steps beyond receptor activation are propagated catalytically, that little substrate is consumed in the initial phase of such reactions, and that forward reaction steps dominate reverse reaction steps for times early in the reaction, the exponential rise in bound receptor concentration, [LR], is accompanied by an explosive increase in $[Ca^{2+}]_i$ with a defined lag phase after stimulus. Fig. 7 *B* shows the calculated $[Ca^{2+}]_i$ signal at each [ATP] shown in Fig. 7 *A*; the calculations assume that the activation of G-proteins by ligand-bound receptors is catalytic, the G-protein activation of PLC is stoichiometric, the production of IP_3 from PIP_2 via PLC is catalytic, and the release of Ca^{2+} from IP_3-sensitive stores is governed by saturation kinetics. The activation of Ca^{2+} release by IP_3 is assumed to be cooperative with $n = 3$ (Meyer et al., 1988). The rise in $[Ca^{2+}]_i$ predicted by this simple model proceeds with a more pronounced delay from time of stimulus ($t = 0$) and with a slower rate of rise with decreasing [ATP] (Fig. 7 *B*), similar to the response seen experimentally. The predicted $[Ca^{2+}]_i$ is given by the multiple integral

$$[Ca^{2+}](t) = K\int_0^t dt'\left\{\int_0^{t'} dt''\int_0^{t''} dt'''[LR](t''')\right\}^n$$

where K is a constant containing reaction rates and concentrations of the signal cascade species and n is the Hill coefficient for IP_3 activation of the IP_3 receptor.

This simplistic model is attractive in that it can predict some aspects of the data reported above. The increasing delay between stimulus and response with decreasing ATP concentration is correctly predicted by the model, as shown in Fig. 7 *B*. Variability from cell to cell in this delay time can also be predicted by the model. Changing the total receptor concentration R_0 in the model leads to a predicted change in the time from stimulus to response, with decreasing R_0 prolonging the delay time and increasing R_0 reducing the delay time at any particular [ATP] (Fig. 7 *C*). At [ATP] = 5 μM, decreasing R_0 10-fold increases the delay time 2.2-fold, whereas increasing R_0 10-fold decreases the delay time 2.1-fold. Similar effects are found when the total concentration of G-protein or PLC is varied. This simple model is relatively insensitive to the choice of the Hill coefficient n for cooperative activation of the IP_3 receptor. Increasing n from 1 to 4 changes the calculated lag time by 20% or less (Fig. 7 *D*). At [ATP] $>$ 1 μM the calculated lag time decreases with increasing n, whereas the opposite is true at [ATP] $<$ 1 μM. The relative lack of sensitivity of the model to the Hill coefficient for IP_3-mediated Ca^{2+} release and the relatively strong sensitivity of the model to the upstream signaling components are consistent with the dominant role of the initiator of the signal cascade (the cell surface nucleotide receptor) found for equilibrium enzyme cascade systems (Stadtman and Chock, 1978).

These results suggest that the cell-to-cell variability seen experimentally can be attributed to variation in the concentration of mediators of the signaling pathway between stimulus and response. This simple model lumps together rate and equilibrium constants along with concentrations of the signal transduction cascade species together in the single constant K, because those parameters are difficult to obtain experimentally. The lack of specific knowledge of the concentrations and kinetics of these components precludes quantitative prediction of absolute $[Ca^{2+}]_i$ by this simple model. Nevertheless, the absolute values of predicted lag times shown in Fig. 7 *B* for $R_0 = 0.1$ compare very favorably with the experimental values in Table 1. This suggests that the $[Ca^{2+}]_i$ signal in response to ATP stimulation results predominantly from a signal transduction cascade and not from an immediate influx of Ca^{2+} through ATP-activated P_{2X} receptor channels. This conclusion is consistent with the electrophysiology results shown here.

Although smooth muscle cells from other tissues express receptor channels that allow Ca^{2+} influx upon ATP stimulus (Bean and Friel, 1990; Benham, 1989; Benham and Tsien, 1987), we have found no evidence for these channels in pig aortic smooth muscle. Furthermore, our finding that heparin injection abolishes the $[Ca^{2+}]_i$ rise in response to ATP stimulation demonstrates that Ca^{2+} influx pathways play an insignificant role in the generation of the $[Ca^{2+}]_i$ response to ATP in these cells. Thus our finding that removal of extracellular Ca^{2+} slows the kinetic response of pig aortic smooth muscle cells (Figs. 4 and 5) suggests that other factors contribute to this modulation. One possibility is that the receptor-ATP interaction is modulated by extracellular $[Ca^{2+}]$. Slowing of the kinetics of receptor-ATP binding would slow the $[Ca^{2+}]_i$ response. Alternatively, enhancement of the loss of Ca^{2+} near the inner surface of the plasma membrane by an increase in Ca^{2+} efflux across the membrane could negatively affect the signaling pathway components downstream from the receptor. For example, the intracellular IP_3 receptor/channel has such a dependence (Iino, 1987; Bezprozvanny et al., 1991; Finch et al., 1991) and could thus participate in the slowing of the response in the absence of extracellular Ca^{2+}.

Control of PLC activity is another potential regulation point. Rapid IP_3 release from synaptosomal microsomes is quantitatively decreased by decreasing extramicrosomal $[Ca^{2+}]$ (Finch et al., 1991). Such a decrease would slow the kinetics of the $[Ca^{2+}]_i$ response. However, tissue slices of bovine tracheal smooth muscle show no decreased IP_3 production in the rapid phase of the response to carbachol (Chilvers et al., 1994). Thus a direct correlation between lowered $[Ca^{2+}]_e$ and decreased PLC activity may or may not explain the slowing of the $[Ca^{2+}]_i$ response with decreased $[Ca^{2+}]_e$ found here.

Several important aspects of the measured delay time between stimulus and response follow directly as a consequence of the nature of the signal transduction pathway, namely a catalytic cascade from receptor activation to rise in $[Ca^{2+}]_i$. In particular, the explosive nature of the $[Ca^{2+}]_i$ response, the ligand concentration dependence of the delay time and rate of rise of the response, the cell-to-cell variability of the response, and the modulation of delay time with change in extracellular Ca^{2+} concentration all are predicted from a simple model mimicking the early phase of the signal cascade. Finer details of the true cell response should be predictable by a more detailed model that includes reverse reactions, long-term dissipative components such as Ca^{2+} pumps, and modulatory contributions of other signaling effectors.

We thank Martyn Evans for his patience and guidance with the electrophysiology work.

This work was supported by the National Institutes of Health (HL 31854), the National Science Foundation (MCB-9304393), the American Cancer Society (FRA-437), and SmithKline Beecham Pharmaceuticals, United Kingdom. Any opinions, findings, conclusions, or recommendations expressed in this material are those of the authors and do not necessarily reflect the views of the specific granting agencies.

REFERENCES

Bean, B. P., and D. D. Friel. 1990. ATP-activated channels in excitable cells. *Ion Channels.* 2:169–203.

Benham, C. D. 1989. ATP-activated channels gate calcium entry in single smooth muscle cells dissociated from rabbit ear artery. *J. Physiol. (Lond.).* 419:689–701.

Benham, C. D., and R. W. Tsien. 1987. A novel receptor-operated Ca^{2+}-permeable channel activated by ATP in smooth muscle. *Nature.* 328: 275–278.

Bezprozvanny, I., J. Watras, and B. E. Ehrlich. 1991. Bell-shaped calcium response curves of Ins(1,4,5)P_3-, and calcium-gated channels from endoplasmic reticulum of cerebellum. *Nature.* 351:751–754.

Boyer, J. L., C. L. Cooper, and T. K. Harden. 1990. [^{32}P]3′-*O*-(4-benzoyl)benzoyl ATP as a photoaffinity label for a phospholipase C-coupled P_{2y}-purinergic receptor. *J. Biol. Chem.* 265:13515–13520.

Cheyette, T. E., and D. J. Gross. 1991. Epidermal growth factor-stimulated calcium ion transients in individual A431 cells: initiation kinetics, and ligand concentration dependence. *Cell Regul.* 2:827–840.

Chilvers, E. R., B. J. Lynch, G. J. Offer, and R. A. J. Challiss. 1994. Effects of membrane depolarization, and changes in intra- and extracellular calcium concentration on phosphoinositide hydrolysis in bovine tracheal smooth muscle. *Biochem. Pharmacol.* 47:2171–2179.

Droogmans, G., G. Callewaert, I. Declerck, and R. Casteels. 1991. ATP-induced Ca^{2+} release and Cl^- current in cultured smooth muscle cells from pig aorta. *J. Physiol. (Lond.).* 440:623–634.

Finch, E. A., T. J. Turner, and S. M. Goldin. 1991. Calcium as a coagonist of inositol 1,4,5-trisphosphate-induced calcium release. *Science.* 252: 443–446.

Goldman, S. J., E. S. Dickinson, and L. L. Slakey. 1983. Effect of adenosine on synthesis and release of cyclic AMP by cultured vascular cells from swine. *J. Cyclic Nucleotide Res.* 9:69–78.

Hamill, O. P., A. Marty, E. Neher, B. Sakmann, and F. J. Sigworth. 1981. Improved patch-clamp techniques for high-resolution current recording from cells and cell-free membrane patches. *Pflügers Arch.* 391:85–100.

Hartley, S. A., and R. Z. Kozlowski. 1997. Electrophysiological consequences of purinergic receptor stimulation in isolated rat pulmonary arterial myocytes. *Circ. Res.* 80:170–178.

Iino, M. 1987. Calcium dependent inositol trisphosphate-induced calcium release in the guinea pig taenia caeci. *Biochem. Biophys. Res. Commun.* 142:47–52.

Kalthof, B., M. Bechem, K. Flocke, L. Pott, and M. Schramm. 1993. Kinetics of ATP-induced Ca^{2+} transients in cultured pig aortic smooth muscle cells depend on ATP-concentration and stored Ca^{2+}. *J. Physiol. (Lond.).* 466:245–262.

Lamb, T. D. 1985. An inexpensive digital tape recorder suitable for neurophysiological signals. *J. Neurosci. Methods.* 15:1–13.

Libby, P., and K. V. O'Brien. 1983. Culture of quiescent arterial smooth muscle cells in a defined serum-free medium. *J. Cell. Physiol.* 115: 217–223.

Linderman, J. J., L. J. Harris, L. L. Slakey, and D. J. Gross. 1989. Charge-coupled device imaging of rapid calcium transients in cultured arterial smooth muscle cells. *Cell Calcium.* 11:131–144.

Mahoney, M. G., C. J. Randall, J. J. Linderman, D. J. Gross, and L. L. Slakey. 1992. Independent pathways regulate the cytosolic [Ca^{2+}] initial transient and subsequent oscillations in individual cultured arterial smooth muscle cells to extracellular ATP. *Mol. Biol. Cell.* 3:493–505.

Meyer, T., D. Holowka, and L. Stryer. 1988. Highly cooperative opening of calcium channels by inositol 1,4,5-trisphosphate. *Science.* 240: 653–656.

Meyer, T., T. Wensel, and L. Stryer. 1990. Kinetics of calcium channel opening by inositol 1,4,5-trisphosphate. *Biochemistry.* 29:32–37.

North, R. A., and E. A. Barnard. 1997. Nucleotide receptors. *Curr. Opin. Neurobiol.* 7:346–357.

Stadtman, E. R., and P. B. Chock. 1978. Interconvertible enzyme cascades in metabolic regulation. *Curr. Top. Cell Regul.* 78:53–95.

Tawada, Y., K. Furukawa, and M. Shigekawa. 1987. ATP-induced calcium transient in cultured rat aortic smooth muscle cells. *J. Biochem.* 102: 1499–1509.

Xiong, Y., S. Xu, and L. L. Slakey. 1991. Modulation of response to adenosine in vascular smooth muscle cells cultured in defined medium. *In Vitro Cell. Dev. Biol.* 27a:355–362.